ULTRASONICALLY ASSISTED DRILLING IN CFRP COMPOSITES

Vaibhav A. Phadnis[1*], Farrukh Makhdum[1], Anish Roy[1], Vadim. V. Silberschmidt[1,]

[1]*Wolfson school of Mechanical and Manufacturing Engineering, Loughborough University, Epinal way, LE11 3TU, UK*
**V.A.Phadnis@lboro.ac.uk*

Keywords: carbon fibre reinforced polymer composite, FE modelling, drilling force, ultrasonically assisted drilling.

Abstract
Ultrasonically assisted drilling (UAD) is a novel machining technique suitable for drilling quasi-brittle materials such as carbon fibre-reinforced polymer composites (CFRP). UAD has been shown to possess several advantages compared to conventional drilling (CD), including reduced thrust forces, diminished burr formation at drill exit and an overall improvement in roundness and surface finish of the drilled hole.
In this paper, numerical and physical experiments are carried out in drilling of CFRP composite for a set of machining parameters, using CD and UAD techniques. The effect of cutting speed on the drilling thrust force is studied for both techniques. A 3D finite element model of conventional drilling of CFRP laminate is developed and later extended to capture dynamic frictional characteristics of UAD. The model accurately captures complex interaction characteristics involved in the process and agrees qualitatively with the experimental results.

1 Introduction

Carbon fibre-reinforced polymer (CFRP) composites are considered materials of the 21st century and have been widely used in structural applications including military and commercial aircrafts due to their excellent properties, such as high specific strength and stiffness, good fatigue and corrosion resistance. For example, the commercial airliner Boeing 787 has approximately 50% of its structural weight comprising of advanced composite materials [1]. The parts made from CFRP are often manufactured to a near-net shape, though additional machining steps are often required to facilitate component assembly. Despite several structural advantages, poor machinability of CFRP composites poses several considerable problems in the fabrication of components, especially in drilling. Furthermore, several studies demonstrated that conventional machining techniques such as drilling gave rise to various damage phenomena such as matrix cracking, fibre pull-out, fibre kinking, fibre-matrix debonding and delamination, resulting in reduced fatigue strength, poor assembly tolerance and abridged structural integrity in CFRP composites [2, 3, 4].

In conventional drilling (CD), the thrust force exerted by the drill during machining has traditionally been regarded as one of the most crucial factor triggering discrete damage phenomena in fibrous composites. It has been observed that if machining can be performed

below a certain critical thrust-force magnitude then damage was observed to be negligible [3, 4]. Thus, a need for a less invasive, alternative drilling technique is recognised to mitigate the discrete damage phenomena and to maintain the structural integrity of CFRP composite structures.

Ultrasonically assisted drilling (UAD) is a non-traditional machining process, where high frequency vibration (typically of frequency $f \geq 20$ kHz) is superimposed on a standard twist drill axially. This ultrasonic vibration is generated by a piezoelectric transducer, specially developed based on drilling requirements (type of workpiece, size of hole, etc.). Several advantages of UAD over CD were reported [5, 6] , including reduction in drilling forces, improved surface finish, reduced tool wear and reduction/elimination of burr formation.

This paper is organised as follows: in Section 2 we discuss our experiments involving CD and UAD techniques to drill holes in CFRP composite using a set of machining parameters with a Ø 6 mm drill. The results for two techniques are compared to show the effectiveness of UAD. In Section 3 we discuss the development and implementation of a 3D finite element model of drilling in CFRP. The model is shown to qualitatively predict various features of the drilling process.

2 Experimental setup and observations

Our drilling experiments were carried out on a universal Harrison M300 lathe machine. The lathe was adequately modified to accommodate an ultrasonic drilling head (Figure. 1). The modification provides a capability to switch between conventional and ultrasonic drilling regimes during a single drilling experiment.

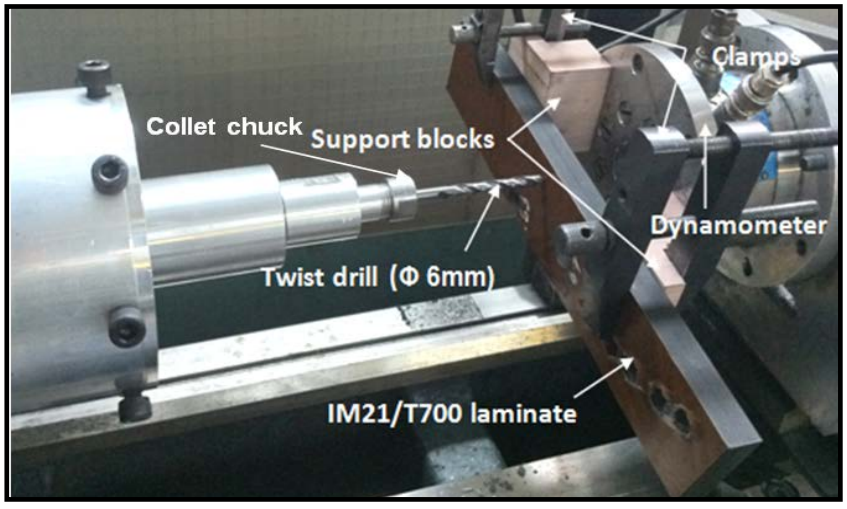

Figure 1. Experimental setup for ultrasonically assisted drilling of M21/T700 composite

Average drilling forces were measured using a Kistler™ dynamometer mounted on an angle plate fixed to the lathe carriage (Fig. 1). A thrust force was recorded using a digital oscilloscope (Picoscope™). For all the drilling experiments reported here, a standard Jobber carbide TiN coated twist drill of Ø 6 mm was used. In UAD, ultrasonic vibrations with a constant resonance frequency of 32.2 kHz and peak-to-peak amplitude of 20 μm were applied on the drill tip. For CD and UAD, the drilling experiments were carried out with five

different cutting speeds and a constant feed rate (Table 1). Each experiment was repeated three times to ensure adequate repeatability of the results.

The studied CFRP was a 15 mm thick laminate (Hexply M21/T700) with individual ply thickness of 0.25 mm. The stack sequence of the composite was $(0/45/90/-45)_{15}$. Elastic properties of a single ply of the laminate in a principal fibre direction were determined with in-house experiments (Table 2). These properties are found to be in agreement with those reported by Hallet and co-workers [7].

Table1. Experimental parameters for drilling of CFRP composite

Drilling parameters		**Magnitude**
Rotational speed	[rpm]	260, 540, 800, 1200, 1700
Feed rate	[mm/min]	50
For UAD only :		
Vibration frequency	[kHz]	32.2
Vibration amplitude (peak to peak, without tool-workpiece contact)	[µm]	20

Table 2: Properties of M21/T700 laminate in fiber direction

E_{11}	E_{22}	ν_{12}	G_{12}
115 GPa	14 GPa	0.29	4 GPa

Average thrust forces measured in UAD and CD at various cutting speed are shown in Table 3. It was noted that, in CD and UAD, the thrust force decreased with an increase in cutting speed. However, the relative thrust force decrease in UAD was noticeably higher (31.1% at 1700 rpm against 15.8 % at 216 rpm) with an increasing cutting speed. Thus, higher rotational speeds are recommended in drilling CFRP.

Table 2.Thrust forces in drilling M21/T70 laminate using CD and UAD techniques

Spindle speed	**Force (N)**		**Average force reduction**
(rpm)	**CD**	**UAD**	**(%)**
260	272±11	229±9	15.8
540	138±12	117±11	15.2
800	125±10	96±8	23.2
1200	121±9	88±10	27.3
1700	119±8	82±13	31.1

3. Finite-Element model of drilling CFRP composite

3.1 Model setup

A 3D finite element model of drilling in a CFRP composite laminate was developed using general-purpose FE software ABAQUS/Explicit, which is ideally suited to model large workpiece deformation and complex tool-workpiece contact conditions. Owing to the complexity of the problem, especially interaction at the drill–workpiece interface and available computing resources, only the first 8 plies of composite are modelled. This simplification adequately captures the drilling thrust forces, as drill flutes fully engage with the workpiece within the first 8 plies, based on the drill geometry.

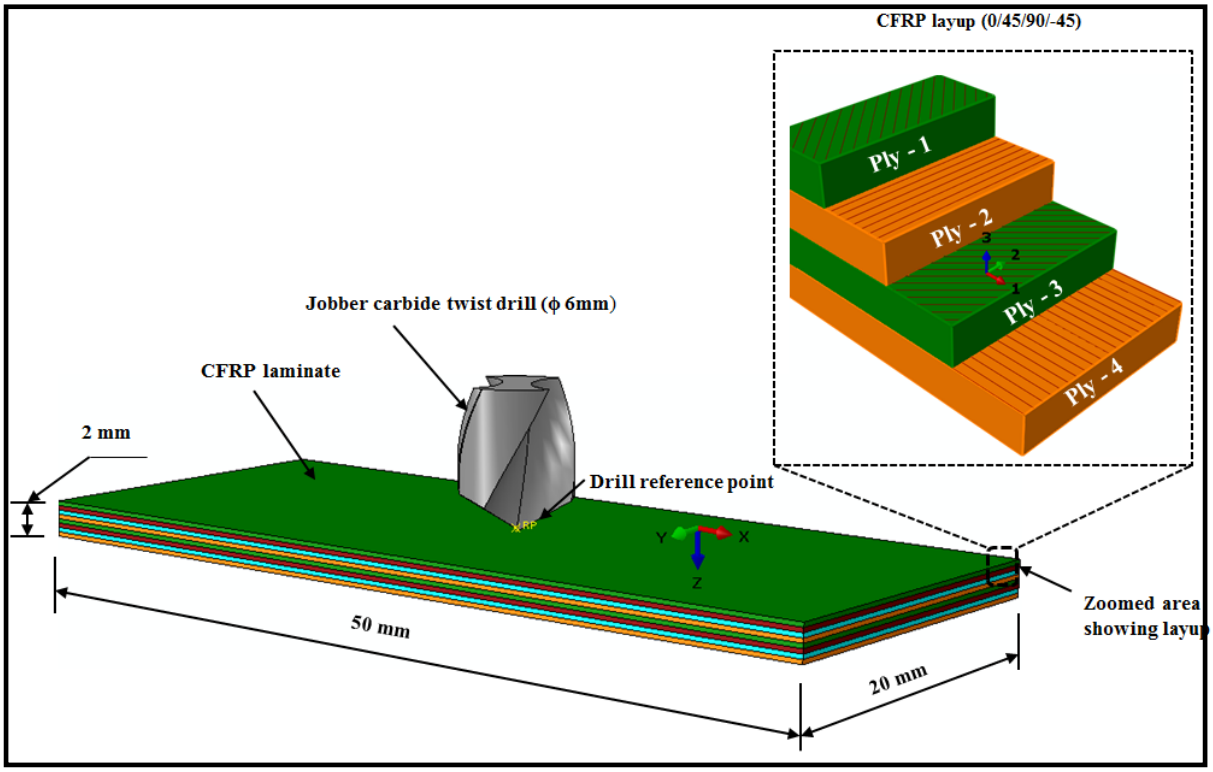

Figure 3. FE model setup for ultrasonically assisted drilling of M21/T700 composite laminate

As shown in Figure 3, a 3D model of a 6 mm twist drill with a point angle of 130° and helix angle of 31° was incorporated in the FE software. The drill was modelled as a rigid body, and the boundary conditions were applied at a reference point on the chisel edge (Figure 3). Dynamic characteristics of the drilling process were accurately modelled by assigning a real mass and rotary inertia at the reference point.

A refined finite element mesh with a minimum size of 10 µm was used at, and in the immediate vicinity of, the workpiece volume to be drilled, while a coarse mesh was employed to discretize the rest of the workpiece volume. The laminate was modelled using 8-node 3D brick elements of type C3D8R with a minimum of 3 elements in *z* direction to adequately capture through-thickness stresses. The drill was modelled with 4-node 3D discrete rigid elements of type C3D4. The CFRP model consists of 200,000 elements while the drill was meshed with 15000 elements, with the smallest element size of 150 µm.

3.2 Drill-workpiece contact and boundary conditions

The parameters used to define contact in our simulations were based on a number of experimental factors such as cutting speed, feed rate, geometry and surface properties.
Contact between the drill and workpiece was modelled using penalty contact conditions and a Coulomb friction constant of magnitude 0.3. Master-slave surface-based contact conditions were incorporated, with the drill surface acting as master and the workpiece surface as slave. [8]. Element deletion was employed to remove heavily distorted elements, which are typical for large deformation solutions. This helped to maintain mesh quality and enabled convergence. The criterion for element deletion is discussed in Section 3.3. Displacement degrees of freedom on the vertical faces of the laminate were constrained, while a rotational displacement was imposed on the drill axis. A linear feed was applied to the workpiece through a reference point on the chisel edge.

In order to investigate the effect of variation in the cutting speed during drilling, several rotational speeds (refer Table 1) and a constant feed rate of 50 mm/min was used in the model. In UAD, ultrasonic vibrations were superimposed at the drill tip in addition to the boundary conditions already discussed. In order to incorporate this periodically changing boundary condition in simulations, instantaneous axial vibration of drill was represented by a sinusoidal wave, which is a function of rotational vibrational frequency (ω) and amplitude of vibration (a). The displacement is represented as

$u_z = a \sin(\omega t)$ Eq. (1)

where, t is the time (in seconds) and u_z is the axial displacement.

Both CD and UAD models required on average 62 hours on a 24 Intel Quad-core processors with 48 GB RAM to complete the analysis. The High Performance Computing (HPC) facility at Loughborough University was used for our purposes.

3.3 Material model

A CFRP laminate was modelled as anisotropic continua; where the fibre and matrix in a ply were represented as 3D homogenized orthotropic material. The ply properties in a principal fibre direction are listed in Table 2. The plies in the model were stacked with appropriate orientations in order to represent the actual CFRP lay-up, as discussed in Section 2. A Hashin's failure criteria [11], used to model damage in long-fibre composites available in ABAQUS [10] for plain-stress elements, was appropriately modified and implemented for 3D solid elements:

$$\text{If } \left(\frac{\sigma_{11}}{S_{11}}\right)^2 + \left(\frac{\sigma_{11}}{S_{12}}\right)^2 + \left(\frac{\sigma_{11}}{S_{13}}\right)^2 = 1,\ d_{ft} = 1 \quad \text{Eq. (2)}$$

$$\text{If } \left(\frac{\sigma_{11}}{X_{1c}}\right)^2 = 1,\ d_{fc} = 1 \quad \text{Eq. (3)}$$

Here $\sigma_{11}, \sigma_{22}, \sigma_{12}, \sigma_{33}$ are the components of stress tensors at an integration point of an element; $d_{ft}, d_{fc}, d_{mt}, d_{mc}$ are the damage variables associated with failure modes in fibre tension, fibre compression, matrix tension and matrix compression, respectively; X_{1c}, X_{2c}, X_{2t} are tensile failure stress in fibre direction, tensile failure stress in direction 2 (transverse to fibre

direction) and compressive failure stress in direction 2, respectively, while S_{11}, S_{12}, S_{13} are shear failure stresses in 1-2, 2-3 and 1-3 planes, respectively. This allows for a better representation of the through-thickness stress variation in the plies.

In order to model matrix damage, a Puck's failure criterion [12] was implemented in the following form:

$$\text{If } \left[\left(\frac{\sigma_{11}}{2X_{1t}}\right)^2 + \frac{{\sigma_{22}}^2}{\left|X_{2t}.X_{2c}\right|} + \left(\frac{\sigma_{12}}{S_{12}}\right)^2\right] + \sigma_{22}\left(\frac{1}{X_{2t}} + \frac{1}{X_{2c}}\right) = 1, \text{ and}$$

$$\sigma_{22} + \sigma_{33} > 0,\ d_{mt} = 1$$

$$\sigma_{22} + \sigma_{33} < 0,\ d_{mc} = 1 \qquad \text{Eq. (4)}$$

as Hashin's criteria could not accurately model damage in a brittle epoxy matrix [9]. The progressive-damage model for fibre and matrix was implemented in ABAQUS/Explicit using a user-defined subroutine (VUMAT). In the FE model of drilling in CFRP laminate employing element deletion mechanism [13], a material point was assumed to fail during deformation when either of the damage variables d ($0 \leq d < 1$) associated with fibre failure modes (tensile or compressive) reached maximum damage (d_{max} =1). The element was removed from the model when this condition was satisfied at all of the element's nodal points. The corresponding damage parameter at all section points of workpiece was calculated using Eqs, (2)-(4).

Tensile strength in longitudinal direction (S_{1t})	2720 MPa
Tensile strength in transverse direction (S_{2t})	111 MPa
Compressive strength in longitudinal direction(S_{1c})	1690 MPa
Compressive strength in transverse direction(S_{2c})	214 MPa
Shear strength in longitudinal direction(S_{1s})	115 MPa

Table 3. Hashin damage parameters used in drilling simulation [9]

3.4 FE results and discussion

3.4.1 Thrust force analysis

Reaction forces at the drill reference point were used to compare the result for both CD and UAD techniques qualitatively with experimental results as shown in Figure 4. The thrust-force magnitude in both cases shows a qualitative match with the experiments. Similar to the experiments, the thrust force decrease in UAD was noticeably higher (28.46 % at 1700 rpm against11.96 % at 216 rpm) with increasing cutting speed.

Thus, a relative force reduction using FE analysis shows a reasonable co-relation with the experimental data with an average error of 5 to7 %, thus demonstrating capabilities of this model to predict experimentally relevant characteristics of the drilling process.

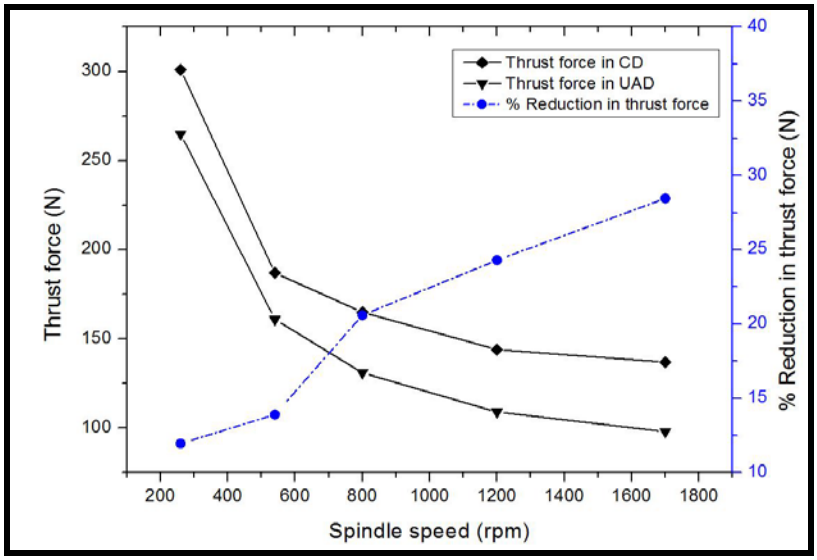

Figure 4. Thrust force analysis using FE modelling for CD and UAD

3.6 Contribution of frictional force in UAD

Several studies on dynamic characteristics of frictional forces at the tool-workpiece contact interface indicate that an increase in the sliding speed between the two surfaces typically leads to a reduction in the effective frictional co-efficient for a given contact pressure [13]. The principal difference between the CD and UAD process lies in the fact that in UAD the axially vibrating drill bit establishes a periodic intermittent contact with the workpiece, opposed to a continuous contact with the tool in CD. Since the tool vibrated at very high frequencies, the relative velocity (sliding velocity) would be significantly higher. This, in turn, would help reduce the effective frictional co-efficient at the interface [7]. Thus, it becomes imperative to study the relative contribution to the overall thrust force from frictional effects at the tool-workpiece interface.

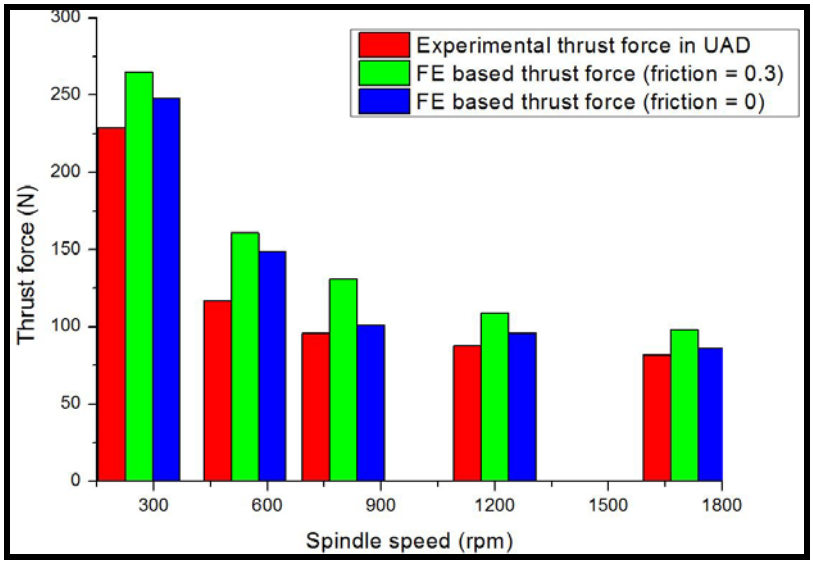

Figure 5. Thrust force analysis with μ = 0.3 and μ = 0 for UAD using FEA

Hence, the effect of dynamic friction was studied by reducing the friction co-efficient from 0.3 to 0 in UAD, for the same set of drilling parameters as discussed before. We noticed a

reduction in the predicted thrust forces for the various drilling speeds studied (Figure 5). We observed that with a zero friction condition, the average thrust force agreed closely with the experimental force reduction. This indicates that further studies are required to accurately determine the effects of dynamic friction, especially in UAD conditions.

4. Conclusions

An experimental study and finite-element simulations were carried out to compare thrust forces obtained using CD and UAD techniques to drill CFRP composite laminate M21/T700. The average thrust force reduction was observed to be as high as 30% at higher cutting speeds in UAD when compared to CD. 3D finite element models of CD and UAD for CFRP composite laminate were developed. The models were validated using experimental results and found to be reasonably accurate in predicting thrust forces for the chosen set of drilling parameters. Additionally, a frictionless contact model was developed where friction between drill bit and the CFRP workpiece was set to zero to study the effect of dynamic friction in UAD;. the model demonstrated better agreement with the experimental results.

References

[1] Hinchcliffe M. Characterisation of bond line porosity, 2011, [04/02/2012]. http://seit.unsw.adfa.edu.au/ojs/index.php/juer/artilce/viewFile/139/95.

[2] Hocheng H, Tsao CC. The path towards delamination-free drilling of composite materials.Journal of Materials Processing Technology, **2–3**, pp. 251-64. (2005).

[3] Capello E. Workpiece damping and its effect on delamination damage in drilling thin composite laminates.Journal of Materials Processing Technology, **2**, pp. 186-95. (2004).

[4] Kim GW, Lee KY. Critical thrust force at propagation of delamination zone due to drilling of FRP/metallic strips.Composite Structures, **2**, pp. 137-41. (2005).

[5] Thomas PNH, Babitsky VI. Experiments and simulations on ultrasonically assisted drilling.Journal of Sound and Vibration, **3–5**, pp. 815-30. (2007).

[6] Liu J, Zhang D, Qin L, Yan L. Feasibility study of the rotary ultrasonic elliptical machining of carbon fiber reinforced plastics (CFRP).International Journal of Machine Tools and Manufacture, **1**, pp. 141-50. (2012).

[7] Hallett SR, Jiang W-G, Khan B, Wisnom MR. Modelling the interaction between matrix cracks and delamination damage in scaled quasi-isotropic specimens.Composites Science and Technology, **1**, pp. 80-9. (2008).

[8] Schön J. Coefficient of friction for aluminum in contact with a carbon fiber epoxy composite.Tribology International, **5**, pp. 395-404. (2004).

[9] Lapczyk I, Hurtado JA. Progressive damage modeling in fiber-reinforced materials.Composites Part A: Applied Science and Manufacturing, **11**, pp. 2333-41. (2007).

[10] ABAQUS version 6.11. User's manual. RI: Hibbitt, Karlsson & Sorensen Inc., (1999)

[11] Hashin Z. Analysis of stiffness reduction of cracked cross-ply laminates. Engineering Fracture Mechanics, **5**, pp. 771-778. (1986).

[12] Puck A, Schürmann H. Faliure analysis of FRP laminates by means of physically based phenomenological models. Composites Science and Technology, **7**, pp. 1045-67. (1998).

[13] Arnoux JJ, Sutter G, List G, Molinari A. Friction experiments for dynamical coefficient measurement. Advances in Tribology: (2011).